International Journal of Mass Spectrometry 276 (2008) 116–126

Contents lists available at ScienceDirect

International Journal of Mass Spectrometry

journal homepage: www.elsevier.com/locate/ijms

Electron capture, femtosecond electron transfer and theory: A study of noncovalent crown ether 1,*n*-diammonium alkane complexes

Anne I.S. Holm, Mikkel K. Larsen, Subhasis Panja, Preben Hvelplund, Steen Brøndsted Nielsen[a,*], Ryan D. Leib[b], William A. Donald[b], Evan R. Williams[b,*], Changtong Hao[c], František Tureček[c,*]

[a] *Department of Physics and Astronomy, University of Aarhus, Aarhus, Denmark*
[b] *Department of Chemistry, University of California at Berkeley, Berkeley, CA 94720-1460, USA*
[c] *Department of Chemistry, Bagley Hall, Box 351700, University of Washington, Seattle, WA 98195-1700, USA*

ARTICLE INFO

Article history:
Received 23 February 2008
Received in revised form 25 April 2008
Accepted 25 April 2008
Available online 3 May 2008

Keywords:
Electron capture dissociation
Electron capture-induced dissociation
18-Crown-6-ether complexes
Diaminoalkane cations
Recombination energies
Excited electronic states

ABSTRACT

Complexes of doubly protonated 1,*n*-diaminoalkanes with one or two molecules of 18-crown-6-ether undergo consecutive and competitive dissociations upon electron capture from a free thermal electron and femtosecond collisional electron transfer from Na and Cs atoms. The electron capture dissociation (ECD) and electron capture-induced dissociation (ECID) mass spectra show very different products and product ion intensities. In ECD, the reduced precursor ions dissociate primarily by loss of an ammonium hydrogen and the crown ether ligand. In ECID, ions from many more dissociation channels are observed and depend on whether collisions occur with Na or Cs atoms. ECID induces highly endothermic C—C bond cleavages along the diaminoalkane chain, which are not observed with ECD. Adduction of one or two crown ethers to diaminoalkanes results in different electron capture cross-sections that follow different trends for ECD and ECID. Electron structure calculations at the B3-PMP2/6-311++G(2d,p) level of theory were used to determine structures of ions and ion radicals and the energetics for protonation, electron transfer, and ion dissociations for most species studied experimentally. The calculations revealed that the crown ether ligand substantially affected the recombination energy of the diaminoalkane ion and the electronic states accessed by electron attachment.

1. Introduction

Ammonium radicals are transient species that formally have nine valence electrons on nitrogen and thus violate the venerable octet rule [1]. Simple ammonium radicals such as $NH_4^{\bullet}$ and a number of alkyl and aryl ammonium derivatives of the $RNH_3^{\bullet}$, $R_2NH_2^{\bullet}$, $R_3NH^{\bullet}$ and $R_4N^{\bullet}$-type have been studied extensively by spectroscopy [2], mass spectrometry [3], and ab initio theory [4], and their fundamental electronic properties and unimolecular dissociations are mostly well understood. Recently, the properties of ammonium radicals have become of increased interest owing to their role in dissociations of biomolecular ions, primarily peptides and proteins, upon reduction by capture of a free electron [5] or transfer from atoms [6] or anions [7] in the gas phase. The interaction of an electron with a multiply protonated protein can result in extensive backbone cleavage from which primary [5], and even tertiary structure information may be obtained [5b–d]. Unlike other ion activation techniques, electron capture can result in retention of labile post-translational modifications [5e–i], which substantially increases the information that may be gained from tandem mass spectrometry.

Chemical recognition in mass spectrometry has shown potential for analytical applications in protein structure elucidation. For example, charged ammonium groups in peptide lysine residues have been found to form gas-phase complexes with crown ethers (CE) [8,9] from which solution-phase structural information may be inferred. For example, 18-C-6-E adduction in solution to various proteins has been used to qualitatively probe the surface accessibility of proteins in solution from the number of CE adducted and the charge state envelopes [9]. Activation of CE adducted peptides by thermal techniques results in loss of the CE prior to covalent bond cleavage [8a,10]. Recently, gas-phase complexes of 18-C-6-E with small doubly charged peptide ions containing one or two lysine residues were studied by collisional electron transfer and the CE had a large effect on the competitive formation of sequence fragments [6a]. Furthermore, collisional electron transfer to a CE adducted dipeptide resulted in backbone fragments, some of which *retained* the noncovalent CE ligand [6a]. These results raised some

---

* Corresponding author. Tel.: +1 206 685 2041; fax: +1 206 685 3478.
E-mail addresses: sbn@phys.au.dk (S.B. Nielsen), williams@cchem.berkeley.edu (E.R. Williams), turecek@chem.washington.edu, turecek@macmail.chem.washington.edu (F. Tureček).

1387-3806/$ – see front matter © 2008 Elsevier B.V. All rights reserved.
doi:10.1016/j.ijms.2008.04.021

fundamental questions about the nature of electronic states that are formed by attaching an electron to CE·ammonium complexes. The present paper reports a systematic study of electron-ion recombination involving 1,*n*-diaminoalkane ions and their complexes with one and two molecules of 18-crown-6-ether. Electron-ion recombination is realized either as electron capture by doubly protonated ions trapped in an ion-cyclotron resonance cell, or as femtosecond electron transfer to doubly protonated ions from alkali metal atoms performed at high ion velocity in a beam experiment. The experimental data are complemented by ab initio and density functional calculations for selected species and interesting comparisons between the two techniques are made.

2. Experimental

2.1. Materials

1,*n*-Diaminoalkanes and 18-crown-6-ether were purchased from Sigma–Aldrich (Milwaukee, WI) and used as received. 1,*n*-Diaminoalkane·CE complexes were prepared in situ by mixing the components in 1:1 or 1:2 molar ratios in methanol or aqueous methanol solutions. Gas-phase ion complexes are represented such that a doubly protonated 1,*n*-diaminoalkane with *m* number of 18-crown-6-ethers (*m* = 1 or 2) is ***n***-*m*CE^{2+}. Species which have undergone deuterium labeling such that they contain *x* number of D atoms will be reported as D$_x$-***n***-*m*CE. The D$_6$-**7**-1CE and D$_6$-**7**-2CE complexes were prepared in CH$_3$OD.

2.2. Methods

Electron capture dissociation (ECD), collision-induced dissociation, and infrared multiphoton dissociation (IRMPD) mass spectra were measured on a Bruker 4.7 T Fourier transform ion cyclotron resonance (FT-ICR) mass spectrometer (Bruker, Framington, MA). The ions were selected by a quadrupole mass filter, accumulated in a hexapole linear trap, and transferred to the ICR cell. The trapped ions were irradiated with an electron pulse for 300–500 ms. The electron energy was adjusted to maximize ECD efficiency. Experiments for measuring the relative efficiency of electron capture for different ions were performed on both 9.4 T [11] and 2.75 T [12] FT-ICR mass spectrometers with similar operating parameters as described elsewhere [5d,13]. Ions of interest were formed by nanoelectrospray of aqueous methanol or methanol solutions, isolated using correlated shot techniques on the 9.4 T instrument or SWIFT on the 2.75 T instrument, and ECD spectra were acquired using 30–40 ms electron radiation times. Data analysis was performed via Xmass 8.1 or Midas Analysis 3.21 for the respective instruments. The ECD efficiency was determined by dividing the sum of all product ion intensities by the sum of all ion intensities present in the spectrum. For experiments in which two precursors were isolated within the same mass spectrum prior to ECD, the corresponding products and precursors are considered separately.

Electron-capture-induced dissociation (ECID) spectra were measured on a sector beam instrument described previously [14]. Doubly protonated ions were generated by electrospray ionization from aqueous methanol solutions that were acidified with 1–5% acetic acid. The ions were accelerated by a 50 kV potential corresponding to 100 keV ion kinetic energies and mass-selected by a magnetic sector. The ion velocities ranged from 1.63×10^5 ms^{-1} for **12**-2CE^{2+} to 3.82×10^5 ms^{-1} for **7**$^{2+}$. Charge transfer was accomplished by collisions with Na or Cs vapor that was admitted to the collision cell to achieve 20–40% conversions of the primary ion beam. The flight times between the collision cell and the electrostatic analyzer were within 3–9 μs for the corresponding charge-reduced ions. This defines the time scale for dissociations taking place after collisional electron transfer.

2.3. Calculations

Standard ab initio calculations were performed using the Gaussian 03 suite of programs [15]. Optimized geometries were obtained by density functional theory calculations using Becke's hybrid functional (B3LYP) [16] and the 6-31+G(d,p) and 6-31++G(d,p) basis sets for closed shell and open-shell species, respectively. Select optimized structures are shown in the pertinent schemes and figures. Complete optimized structures of all local minima and transition states can be obtained from the corresponding author (F. T.) upon request. Spin unrestricted calculations were performed for all open-shell systems. Stationary points were characterized by harmonic frequency calculations with B3LYP/6-31+G(d,p) or 6-31++G(d,p) as local minima (all real frequencies) and first-order saddle points (one imaginary frequency). The calculated frequencies were scaled with 0.963 [17] and used to obtain zero-point energy corrections, enthalpies, and entropies. The rigid-rotor-harmonic-oscillator (RRHO) model was used in thermochemical calculations except for low frequency modes where the vibrational enthalpy terms that exceeded 0.5 RT were replaced by free internal rotation terms equal to 0.5 RT.

Improved energies were obtained by single-point calculations that were carried out with B3LYP and Møller–Plesset theory (second-order, frozen core) using the 6-311++G(2d,p) split-valence triple-ζ basis set furnished with polarization and diffuse functions. For the molecular system of the **7**-1CE size, the larger basis set comprised 1530 primitive Gaussians and the MP2 calculations required over 50 GB of scratch space. The spin unrestricted formalism was used for calculations of open-shell systems. Contamination by higher spin states was modest, as judged from the expectation values of the spin operator $\langle S^2 \rangle$ that were $\leq$0.76 for UB3LYP and $\leq$0.78 for UMP2 calculations. The UMP2 energies were corrected by spin annihilation [18] that reduced the $\langle S^2 \rangle$ to close to the theoretical value for a pure doublet state (0.75). Spin annihilation lowered the total MP2 energies by 6 millihartree (15.7 kJ mol^{-1}, root mean square deviation) for local energy minima and transition states. The B3LYP and MP2 energies calculated with the large basis set were combined according to the B3-MP2 scheme, as described previously [19].

Vertical excited state energies were calculated with time-dependent density functional theory [20] using the B3LYP functional and the 6-311++G(2d,p) basis set. Atomic spin and charge densities were calculated using the natural population analysis (NPA) method [21]. Excited state wave functions were constructed as linear combinations of virtual orbitals with expansion coefficients obtained from TD-B3LYP/6-311++G(2d,p) calculations.

3. Results and discussion

3.1. Ion formation

Electron capture and transfer were studied for a series of cations either free or in complexes with one or two molecules of CE. Diaminoalkanes with chain lengths from *n* = 4 to 12 were investigated. Doubly protonated ions were produced by electrospray ionization of free amines or in mixtures with CE. The ions are denoted as ***4***$^{2+}$–***12***$^{2+}$ for free diammonium, ***4***-1CE^{2+}–***12***-1CE^{2+} for complexes with one molecule of CE, and analogously, ***4***-2CE^{2+}–***12***-2CE^{2+} for the complexes with two CE molecules.

The efficiency for the formation of doubly protonated ions by electrospray was found to increase with the diaminoalkane chain length and the number of crown ether molecules in the com-

Table 1
Calculated proton affinities and gas-phase basicities[a,b]

Species/reaction	$\Delta H^\circ_{g,298}$ (PA)	$\Delta G^\circ_{g,298}$ (GB)
$(1,7\text{-Heptanediamine}+2H)^{2+} \rightarrow (1,7\text{-heptanediamine}+H)^{+}+H^{+}$	690	672
$(1,12\text{-Dodecanediamine}+2H)^{2+} \rightarrow (1,12\text{-dodecanediamine}+H)^{+}+H^{+}$	749	735
$(\boldsymbol{4}\text{-1CE}+2H)^{2+} \rightarrow (\boldsymbol{4}\text{-1CE}+H)^{+}+H^{+}$	734	700
$(\boldsymbol{5}\text{-1CE}+2H)^{2+} \rightarrow (\boldsymbol{5}\text{-1CE}+H)^{+}+H^{+}$	756	723
$(\boldsymbol{7}\text{-1CE}+2H)^{2+} \rightarrow (\boldsymbol{7}\text{-1CE}+H)^{+}+H^{+}$	790	755
18-Crown-6-ether	954 (967)[c]	914 (910)[c]
1,7-Heptanediamine	987 (998)[c]	942 (945)[c]
Pyridine	928 (930)[c]	896 (898)[c]
CH_3OH	750 (754)[c]	720 (725)[c]

[a] In units of kJ mol^{-1}.

[b] From combined B3LYP and MP2/6-311++G(2d,p) calculations and B3LYP/6-31+G(d,p) zero-point energies, enthalpies, and entropies.

[c] Experimental PA and GB values in parentheses are from reference [23].

plex. For $\boldsymbol{4}^{2+}$ through $\boldsymbol{7}^{2+}$, electrospray did not produce sufficient populations of doubly protonated diaminoalkanes to allow ECD spectra to be obtained. Coulomb repulsion in the doubly protonated ions increases with decreasing chain length and results in a lower apparent gas-phase basicity with decreasing ion size [22]. Although $\boldsymbol{5}^{2+}$ can be formed [22a], proton transfer to methanol is rapid. The proton transfer reactivity decreases with increasing chain length; for $\boldsymbol{7}^{2+}$, proton transfer to methanol occurs at a rate of 7×10^{-12} cm^3 mol^{-1} s^{-1} whereas this value for $\boldsymbol{8}^{2+}$ is substantially less [22a].

Proton affinities and gas-phase basicities (GB) were calculated using B3-MP2 for several species of interest, as summarized in Table 1. The majority of the calculated PA or GB values were within 4–5 kJ mol^{-1} of reliable tabulated values [23], e.g., those for methanol, pyridine, and 1,7-diaminoheptane. CEs solvate protons and ammonium ions and thus increase the stability of ion complexes in the gas phase. The PA of 18-crown-6-ether is important for the energetics of the dissociation of these complexes. The calculated PA of 18-crown-6-ether (954 kJ mol^{-1}) significantly differs from the experimental value from ref. [23] (967 kJ mol^{-1}, Table 1). We note that the original experimental datum resulted in $\Delta G^\circ_{g,600} = 11 \pm 8$ kJ mol^{-1} for proton exchange with pyridine (Eq. (1)) at a temperature of 600 K [24], and the PA value was later extrapolated using an entropy estimate [23]. Experimental difficulties were noted by Mautner that were due to ion decomposition reactions [24]. Our calculations of the thermochemistry of Eq. (1) reproduce the experimental $\Delta G^\circ_{g,600}$ but provide a lower PA because of smaller entropy correction.

$$(\text{18-Crown-6-ether} + H)^{+} + \text{pyridine} \rightarrow \text{18-crown-6-ether} + (\text{pyridine} + H)^{+} \qquad (1)$$

$\Delta H^\circ_{g,298} = 26.7$ kJ mol^{-1}; $\Delta G^\circ_{g,298} = 18.6$ kJ mol^{-1}; $\Delta G^\circ_{g,600} = 11.4$ kJ mol^{-1}.

Since our calculations reproduce well both the experimental PA of pyridine (928 kJ mol^{-1} calculated, 930 kJ mol^{-1} experimental, Table 1) [23] and the ΔG for the (Eq (1)) reaction, we believe that the calculated PA = 954 kJ mol^{-1} is to be preferred over the extrapolated experimental estimate.

The complexes $\boldsymbol{4}$-1CE^{2+} and $\boldsymbol{5}$-1CE^{2+} were also difficult to generate by electrospray, as the majority of ions being formed were singly protonated complexes. The formation of doubly protonated complexes $\boldsymbol{4}$-2CE^{2+}–$\boldsymbol{12}$-2CE^{2+} was facile, presumably due to the decreased proton transfer reactivity of the CE complexated ammonium. The ions generated by electrospray were used for electron capture and electron transfer experiments. The mass spectrometric data are first described separately and then the results are compared.

3.2. *Diaminoalkane complexes with one and two CE molecules*

Electron capture of doubly protonated diaminoalkane·CE is illustrated by the ECD spectrum of $\mathbf{7}$-1CE^{2+} (Fig. 1). The spectrum shows a very weak peak at m/z 395 corresponding to the charge-reduced ion that has lost one hydrogen atom, which is denoted as M$^+$, and singly charged fragments originating from protonated CE, e.g., $C_8H_{17}O_4$ at m/z 177.112, $C_6H_{13}O_3$ at m/z 133.085, and $C_4H_9O_2$ at m/z 89.059. These ions also arise by CID and IRMPD of protonated CE and diammoniumalkane·CE complexes, as determined by independent measurements and shown in Fig. S1 (Supplement), although the fragment relative intensities differ for IRMPD and ECD. Complementary ions in the ECD mass spectrum that correspond to $\mathbf{7}^+$ were found at m/z 131.154, denoted as A$^+$, and m/z 114.127 by loss of ammonia from A$^+$. The formation of the major ECD fragments can be accounted for by dissociations shown in Scheme 1, which were further corroborated by deuterium labeling. The ECD spectrum of a mixture of D_6-$\mathbf{7}$-1CE^{2+} (m/z 201.178) and D_5-$\mathbf{7}$-1CE^{2+} (m/z 200.675, from incomplete exchange) showed fragments at m/z 400.341 and 399.337 due to loss of an ammonium D from the charge-reduced complex, and the D_5-$\mathbf{7}^+$ at m/z 136.186 and D_4-$\mathbf{7}^+$ m/z 135.179 (Fig. 2). Interestingly, the relative intensity of the deuterated M$^+$ ions from D_6- and D_5-$\mathbf{7}$-1CE^{2+} was ca. 10-fold greater than that for the non-deuterated ones from $\mathbf{7}$-1CE^{2+}, indicating a substantial kinetic isotope effect on their consecutive dissociation.

The ECD spectra of $\boldsymbol{4}$-2CE^{2+} through $\boldsymbol{12}$-2CE^{2+} were simple and are represented by the spectrum of $\mathbf{7}$-2CE^{2+} (Fig. 3). This showed a major fragment at m/z 395.302 (ion M$^+$) corresponding to a

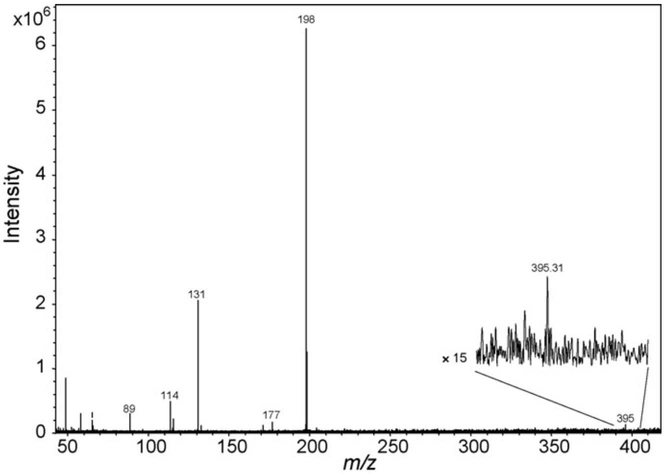

Fig. 1. Electron capture dissociation mass spectrum of $\mathbf{7}$-1CE^{2+}. The precursor ion is at m/z 198. Inset shows the expanded m/z 395 region.

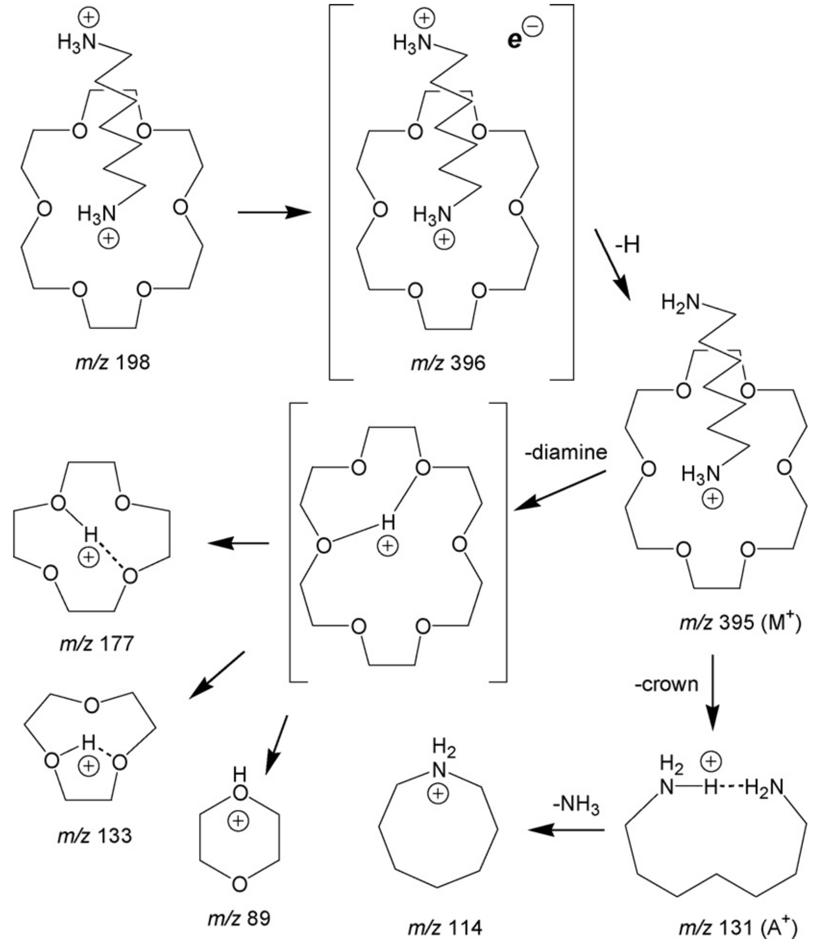

Scheme 1.

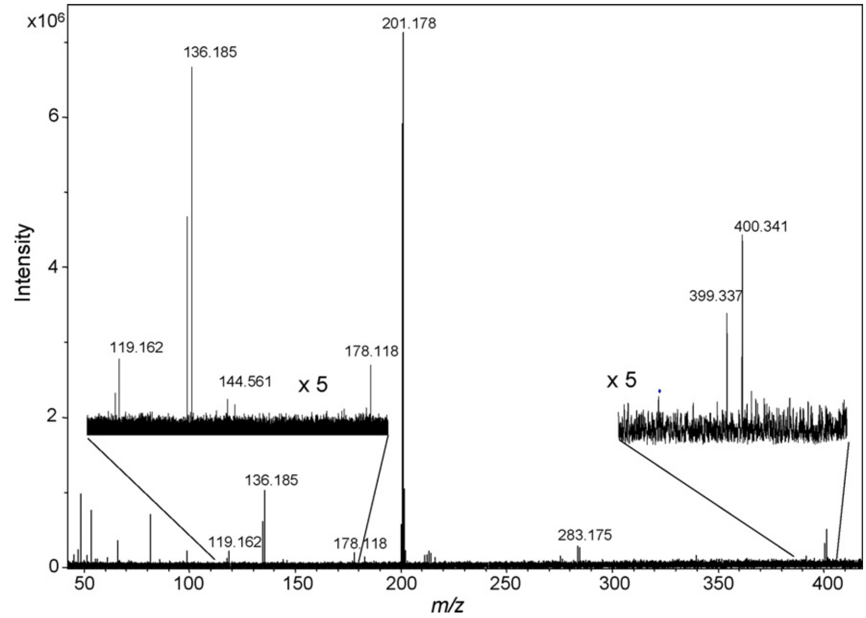

Fig. 2. ECD mass spectra of D_6-**7**-1CE^{2+}. Insets show expanded regions of ECD fragments.

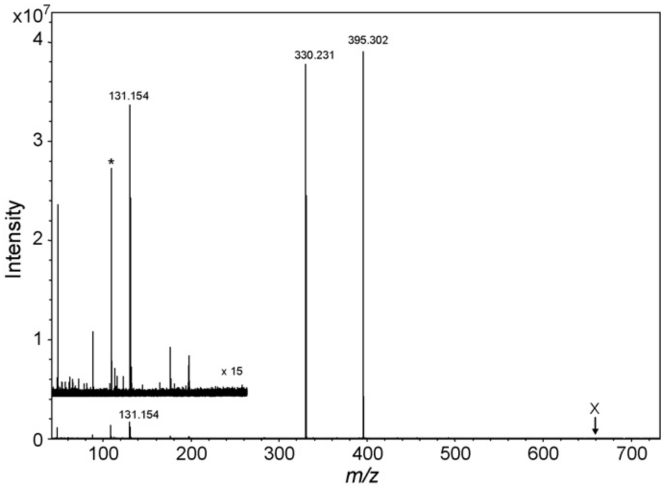

Fig. 3. ECD mass spectrum of **7**-2CE^{2+}. The precursor ion is at m/z 330.231. The arrow with X indicates the position of the missing charge-reduced **7**-2CE^{+} ion at m/z 660.46. The peak labeled with an asterisk is a third harmonics of the m/z 330 peak. Inset shows the expanded low mass region.

combined loss of an H atom and one CE molecule from the charge-reduced complex. Less abundant fragments appeared at m/z 177, 133, and 89 that originated from the protonated CE, and at m/z 131 for protonated **7**$^{+}$ (ion A^{+}).

3.3. Electron transfer to free diammonium cations

Charge transfer collisions with alkali metal atoms were first studied for **7**$^{2+}$ and ***12***$^{2+}$. The ECID spectra showed some common features that are exemplified by the Na-ECID spectrum of **7**$^{2+}$ at m/z 66 (Fig. 4). The spectrum does not show an intact charge-reduced ion at m/z 132. The major charge-reduced fragment is at m/z 131 corresponding to **7**$^{+}$ formed by loss of a hydrogen atom. Other, less abundant, fragments appear at m/z 115 (loss of NH_3), 114 (combined loss of H and NH_3), 98 (loss of two NH_3 molecules), and 97 (combined loss of H and two NH_3 molecules). Interestingly, the spectrum also shows backbone fragments due to C—C bond cleavages, e.g., cation-radicals at m/z 101 (loss of CH_2NH_3), 87 (loss of $CH_2CH_2NH_3$), closed-shell amine cations at m/z 72, 44, 30 ($CH_2NH_2^+$), and 18 (NH_4^+), and hydrocarbon cations at m/z 69, 55, 41, and 39. The formation of cation-radical fragments is interesting because it indicates high-energy dissociations occurring either in the charge-reduced ion or in the m/z 131 and m/z 115 fragments. Note that C—C backbone fragmentation was previously observed for radicals derived from singly protonated butane and hexane 1,n-diamines under conditions of endothermic electron transfer at 8 keV [31]. Hence the donor–acceptor energy balance does not seem to play a dominant role in electron transfer collisions at keV kinetic energies [25].

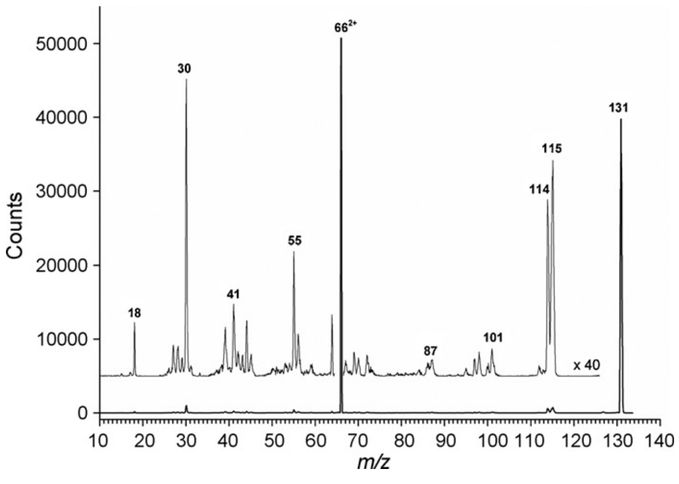

Fig. 4. ECID mass spectrum of **7**$^{2+}$, collisions with Na.

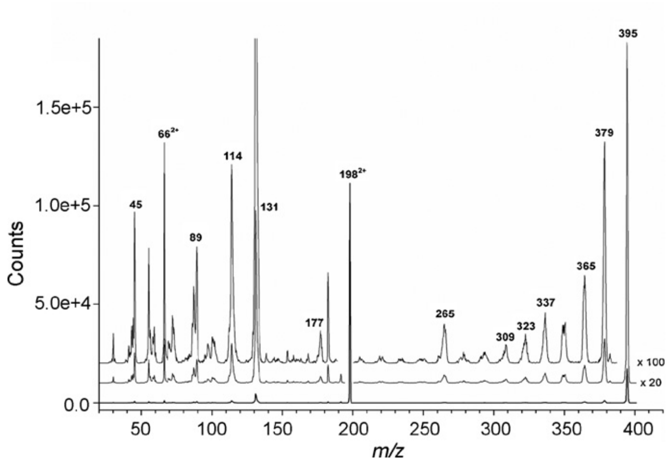

Fig. 5. ECID mass spectrum of **7**-1CE^{2+}, collisions with Na.

ECID of ***12***$^{2+}$ with Na and Cs atoms gave similar results. The spectra did not show intact charge-reduced ions at m/z 202, while the major fragment in each case was at m/z 201 due to loss of a hydrogen atom. The other less abundant fragments were at m/z 185 (loss of NH_3), 184 (combined loss of H and NH_3), and 157 (combined loss of H and two NH_3 molecules). Backbone dissociations gave rise to a cation radical at m/z 171 (loss of CH_2NH_3) and closed-shell cations at m/z 156, 142, 128, 114, 44, and 30, as well as the usual hydrocarbon fragments at m/z 83, 69, 55, and 41. Overall, the spectra were fairly insensitive to the identity of the electron donor (Na or Cs) and the charge transfer conversion, although some differences deserve a note. The abundance ratios for the m/z 201 (loss of H) and m/z 184,185 (loss of NH_3) fragments were $[M-H]/[M-NH_3]=30$ for charge transfer with Na at 41% conversion and 60 for charge transfer with Cs at 34–87% conversions from several measurements made on different days. The peaks in the Cs-ECID spectra are broader, so the m/z 185 and 184 peaks were not resolved. The spectra indicate that electron transfer from Cs favored loss of H over loss of NH_3 even more than did collisions with Na. The energetics of electron transfer to diammonium dications and their dissociations are addressed later in the paper.

3.4. Electron transfer to diammonium complexes with one or two crown ether molecules

Charge transfer collisions with Na and Cs were studied for complexes of diaminoalkanes ($n=6$, 7, and 12) with one or two CE molecules. The spectra of single CE complexes are represented by the Na-ECID spectrum of **7**-1CE^{2+} at m/z 198 (Fig. 5). The spectrum does not display an intact charge-reduced ion at m/z 396. The most abundant fragment is at m/z 395 (M^{+}) due to loss of a hydrogen atom. Other fragments appear at m/z 379 (loss of NH_3), 265 (protonated CE by loss of H and **7**). 131 (**7**$^{+}$, A^{+}), and 114 (loss of NH_3 from A^{+}). In addition, the spectrum shows an ion series at m/z 365, (351 and 350), 337, 323, 309, 294 and 295, 280, etc., that arise by C—C bond dissociations at various positions of the diamine backbone in the complex. Fragments originating from dissociations of protonated CE (m/z 265) appear at m/z 177, 89, and 45.

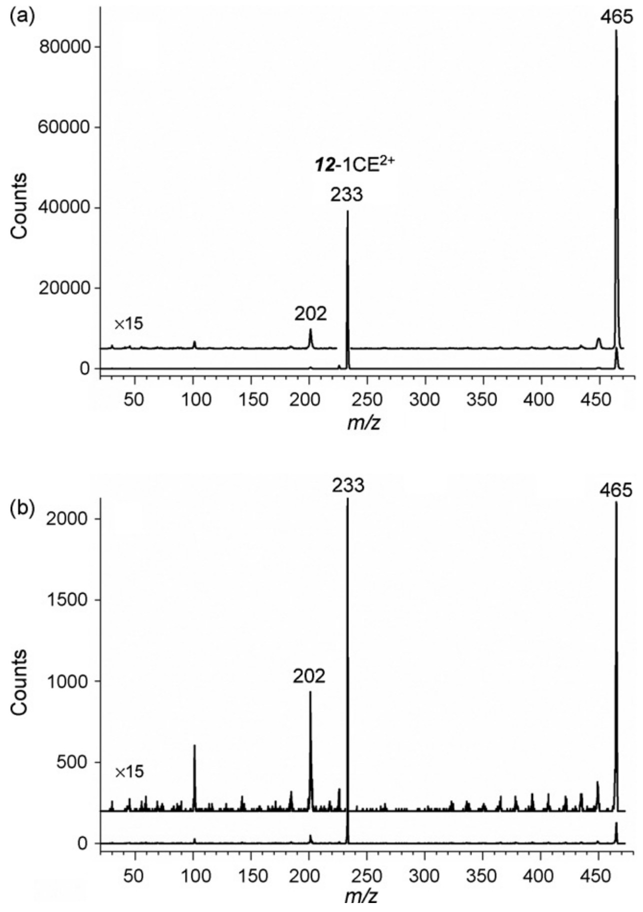

Fig. 6. ECID spectra of ***12***-1CE^{2+} (a) collisions with Cs and (b) collisions with Na.

An interesting effect was observed for ECID with Cs and Na. Collisions with Cs resulted in [M – CE]$^+$/[M]$^+$ ratios which were in general lower than those obtained for collisions with sodium, indicating less dissociation. For example, with ***12***-1CE^{2+} these ratios were 0.1 and 0.4 for Cs and Na, respectively (Fig. 6), and a qualitatively similar trend was observed for ***7***-1CE^{2+}. Since the loss of the CE ligand from M$^+$ is endothermic (see Table 3 and discussion below), the ECID data indicate that M$^+$ ions produced by electron transfer from Cs were less excited than those formed by collisions with Na. However, removal of an electron from Cs requires 1.25 eV less energy than from Na, and so resonant electron transfer to the doubly charged CE complex should be more exothermic for Cs. In addition, the center of mass (COM) collision energy with Cs is greater than that for Na, although any effects of the COM on internal energy deposition in these ECID experiments should be minor. Both of these factors, however, should result in more energy deposited into the ECID products with Cs. This effect is discussed later in conjunction with the dissociation energetics.

Collisional charge transfer from Na and Cs to dication complexes with two CE molecules was studied for $n = 6$, 7, and 12, and the ECID spectra are represented by that of ***7***-2CE^{2+} (*m*/*z* 330, Fig. 7). The spectrum shows a very weak peak at *m*/*z* 659 due to loss of an H atom from the charge-reduced ion, and its dissociation products due to fragmentation of the CE (*m*/*z* 437, and 408). A major fragment is found at *m*/*z* 395 due to loss of an H atom and one CE molecule. The spectrum also shows a series of fragments at *m*/*z* 379, 365, 351, 337, 323, etc., that arise by C—C bond dissociations in the ***7***$^+$ chain in a complex with one CE molecule. Protonated CE at *m*/*z* 265 is much weaker than ***7***$^+$ at *m*/*z* 131, consistent with the higher basicity of the diamine. CE fragments appear at *m*/*z* 177, 89, and 45.

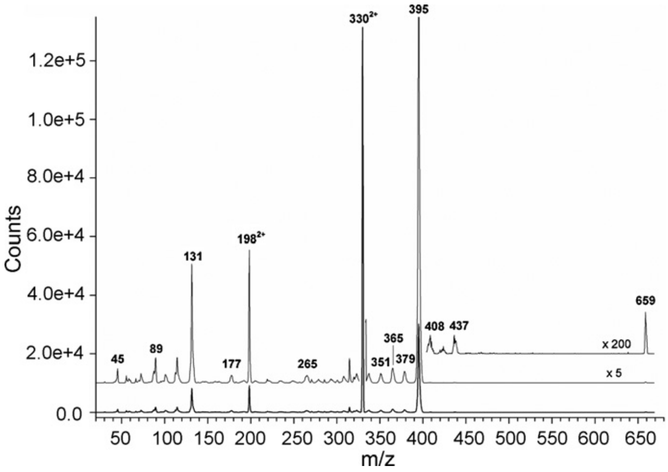

Fig. 7. ECID mass spectrum of ***7***-2CE^{2+}, collisions with Na.

3.5. Relative electron capture and transfer efficiencies

As described above, ECD of ***12***-1CE^{2+} and ***12***-2CE^{2+} ions resulted in a fragment ion that has lost a hydrogen atom and a single CE ligand. Fragment ions corresponding to the loss of a single hydrogen atom or the loss of both CE from the doubly adducted species were not observed (<0.5%) under these conditions. To compare the ECD efficiency of ions with one or two CE adducted, these ions were isolated and ECD spectra simultaneously acquired with both ions in the cell. ECD efficiencies of 6.8 ± 0.2% and 11.0 ± 1.3% were obtained for the ***12***-1CE^{2+} and ***12***-2CE^{2+} adducts, respectively, on the 2.7 T FT/ICR mass spectrometer. Values of 9.7 ± 0.2% and 15.9 ± 1.5% were obtained for these respective ions on the 9.4 T instrument. Although the absolute ECD efficiencies depend on many experimental parameters and can be varied over a wide range, the relative difference in ECD efficiencies for these two ions was the same over a reasonable range of experimental conditions. The 1.6-fold greater ECD efficiency for the two crown ether adduct versus the one crown ether adduct measured with two different instruments and two different isolation methods (and different isolation waveforms) indicates that the difference is intrinsic to the ions rather than an artifact of ion isolation which might result in differing residual excitation of these ions. Similar results were obtained for ***7***-1CE^{2+} and ***7***-2CE^{2+}.

ECID efficiencies of ***12***$^{2+}$, ***12***-1CE^{2+}, and ***12***-2CE^{2+} measured under conditions of constant precursor velocity (1.9×10^5 m/s) were 20%, 15%, and 9 ± 1%, respectively. In contrast to ECD, the ECID efficiency is lower for the complex with two crown ether ligands versus the one crown ether adduct. The nature of this difference is not clear although it does indicate that different factors affect the cross-sections under the conditions of free electron capture and femtosecond collisional electron transfer.

3.6. Ion and radical structures and energetics

The doubly charged 1,*n*-diaminoalkane ions adopt fully extended all-anticonformations induced by Coulomb repulsion between the charged groups, as shown for ***7***$^{2+}$ (Fig. 8). The distance between the N atoms in the fully optimized structures was 6.4, 7.6, 10.2, and 16.6 Å for $n = 4$, 5, 7, and 12, respectively. Regarding the complexes, the CE ligand forms three non-equivalent hydrogen bonds to the internally solvated ammonium group, as shown for ***7***-1CE^{2+} (Fig. 8) and likewise for ***4***-1CE^{2+} and ***5***-1CE^{2+}. The distance

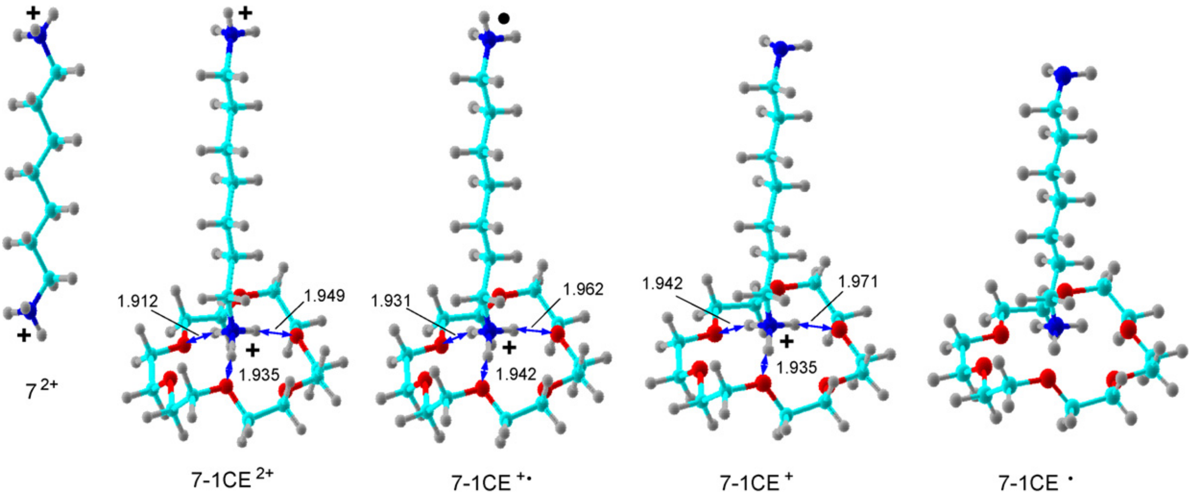

Fig. 8. B3LYP/6-31+G(d,p) optimized structures of 1,7-diaminoheptane ions and complexes.

between the N atoms in ***4***-1CE^{2+}, ***5***-1CE^{2+}, and ***7***-1CE^{2+} was calculated to be 6.4, 7.6, and 10.2 Å, respectively, which is essentially the same as in the respective free diaminoalkane ions. The ***12***$^{2+}$CE complex and those with two CE ligands were too large to be treated adequately by high-level ab initio calculations.

Ion recombination energies (RE) are perhaps the most important parameters characterizing ion-electron recombination and electron transfer from atomic targets and their values can be accurately measured using ion nanocalorimetry [13,26]. Here, both adiabatic (RE_a) and vertical (RE_v) recombination energies were calculated for several singly and doubly charged ions of interest and are reported as absolute values, $|RE_a| = IE_a$, where IE_a is the adiabatic ionization energy. Adiabatic recombination energies express the energy difference between the ground electronic and vibrational state of the charged species and those of its charge-reduced or neutralized radical counterpart. They involve the corresponding potential energy minima and include zero-point vibrational energy corrections for both species. A particular feature of charge reduction in doubly protonated diaminoalkanes is the removal of coulomb repulsion between the charges in the product that allows for chain folding to form conformers with intramolecular hydrogen bonds that would be unstable in doubly charged precursor ions. These changes contribute to differences between the adiabatic and vertical recombination energies for these ions. Vertical recombination energies are obtained as the energy upon attachment of an electron to the frozen optimized geometry of the ion in its ground electronic and vibrational state. The difference between the RE_a and RE_v is used as a measure of vibrational excitation of the charge-reduced species upon vertical electron transfer [27]. Since the charge-reduced species is not in the potential energy minimum, zero-point corrections are not applicable for RE_v. Recombination energies for the formation of the N-th excited electronic state of the charge-reduced species $(RE_v)_N$, are obtained from the RE_v and the pertinent radical vertical excitation energy from the singly occupied molecular orbital (SOMO, $\boldsymbol{X}$) to the N-th state $(RE_v)_N = RE_v - \Delta E(\boldsymbol{X} \rightarrow \boldsymbol{N})$.

The adiabatic and vertical recombination energies depend on the diaminoalkane chain length that determines the distance between the charged ammonium groups and thus affects the Coulomb energy which is released upon electron attachment. The calculated data for 1,n-diaminoalkane ions and their CE complexes are summarized in Table 2. Both RE_v and RE_a can be least-squares fitted in Coulomb-like formulas, e.g., for 1,n-diaminoalkane ions (Eq. (2)),

$$RE_v(\mathrm{eV}) = 3.83 + \frac{14.4}{0.84r} \tag{2}$$

where r is the distance in Angstroms between the ammonium nitrogen atoms in the dication. The additive constant (3.83 eV) represents the recombination energy at an infinite charge distance, such as in a monocation, e.g., $RE_v = 3.79$ eV for 1-ammoniumheptane. The adiabatic recombination energies determine the energy deposited in the charge-reduced cations upon electron capture. The RE_v are important for collisional electron transfer which occurs as a vertical process. Note that the RE_v for the short diaminoalkane ions exceed the IE of Na (5.139 eV) and Cs (3.894 eV) making the electron transfer exothermic. The RE_v for ***12***$^{2+}$ is slightly lower than IE (Na). Nevertheless, the ions that are charge-reduced upon collisions with Na completely dissociate, consistent with the behavior of simple ammonium radicals formed by endoergic collisional electron transfer [3d–n].

The RE of ***4***-1CE^{2+} through ***7***-1CE^{2+} are 0.87 and 0.60 eV lower than those of the respective free diaminoalkane cations (Table 2). The crown-ether effect on the RE is probably due to the polarization of the crown-ether ligand by hydrogen bonding to the inner

Table 2
Calculated adiabatic and vertical recombination energies[a]

Ion	RE_a[b,c]	RE_v[b]
$CH_3NH_3^+$	4.31 (4.24)[d]	
(1-Heptaneamine + H)$^+$	3.96	3.79
$H_2N(CH_2)_7NH_3^+$	3.26	3.06
(18-Crown-6-ether + H)$^+$	2.19	2.05
(18-Crown-6-ether + CH_3NH_3)$^+$	1.74	–
(18-Crown-6-ether + $H_3N(CH_2)_7NH_2$)$^+$	1.85	–
(1,4-Butanediamine + 2H)$^{2+}$	6.67	6.44
(1,5-Pentanediamine + 2H)$^{2+}$	6.32	6.11
(1,7-Heptanediamine + 2H)$^{2+}$	5.72	5.61
(1,12-Dodecanediamine + 2H)$^{2+}$	5.22	5.02
4-1CE^{2+}	5.80	–
5-1CE^{2+}	5.60	–
7-1CE^{2+}	5.12	5.08

[a] Absolute values in units of electron volts.

[b] From combined B3LYP and PMP2/6-311++G(2d,p) single-point calculations.

[c] Including B3LYP/6-31++G(d,p) zero-point energies.

[d] CCSD(T)/aug-cc-pVTZ value from reference [28].

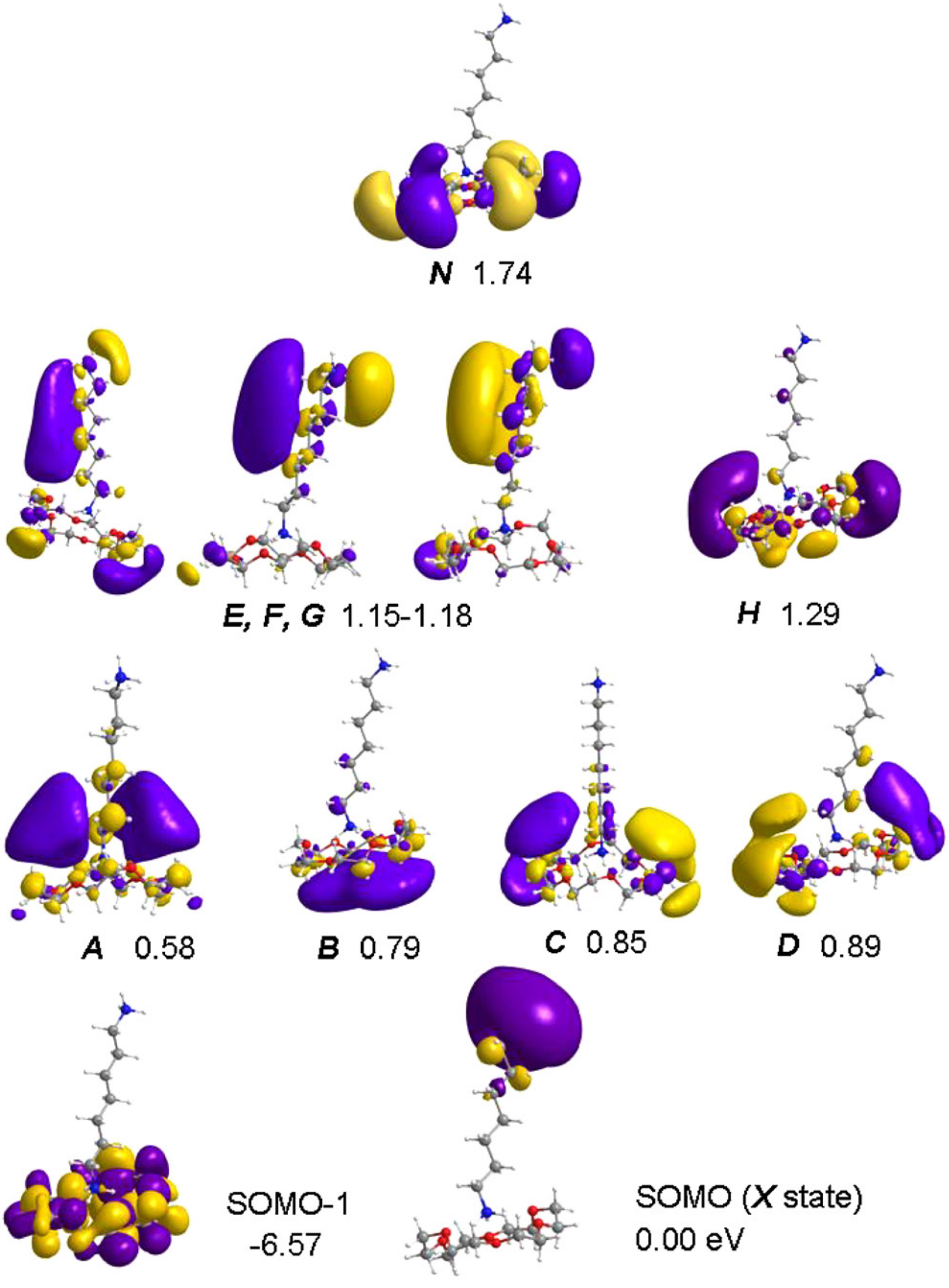

Fig. 9. Electronic states in **7**-1CE$^{\bullet+}$. Excitation energies in eV are from TD-B3LYP/6-311++G(2d,p) single-point calculations.

ammonium group. This results in delocalization of the positive ammonium charge onto atoms which are more remote from the outer (free) ammonium, thus diminishing the Coulomb energy release upon electron attachment.

CE complexation also has a pronounced effect on the recombination energy of the ammonium group, as shown for complexes of methylammonium and 7-aminoheptyl-1-ammonium (Table 2). The CE-complexated ammonium cations show conspicuously lower recombination energies than the free ammonium cations, e.g., ΔRE = −2.57 and −1.41 eV for methylammonium and 7-aminoheptyl-1-ammonium. The calculations indicate that the *ground electronic state* of charge reduced 1,*n*-diaminoalkane·CE complexes should retain the inner, CE-coordinated, ammonium ions while the electron enters the outer free ammonium group converting it into a hypervalent ammonium radical.

Analysis of electronic states in charge-reduced **4**-1CE$^{\bullet+}$ through **7**-1CE$^{\bullet+}$, as represented by the latter species in Fig. 9, corroborates this hypothesis. Fig. 9 shows the SOMO (***X*** state) as being an ammonium 3 s Rydberg [28], which is delocalized over the outer ammonium group, but has no significant odd-electron density in the CE-complexated ammonium. Accordingly, the latter carries 60% of the charge in **7**-1CE$^{\bullet+}$ with additional 12% delocalized over the CE ligand. The outer, reduced, ammonium group carries 91% of spin density and has a total of −0.22 negative atomic charge. The electron distribution changes rather dramatically in the low-lying excited electronic states of **7**-1CE$^{\bullet+}$ (Fig. 9). Of these, the ***A*** and ***B*** states can be characterized as 3s-type Rydbergs delocalized about the alkane chain α-CH_2 group and the CE ligand, respectively. The higher ***C*** through ***H*** states resemble symmetry-adjusted 3p and 3d Rydberg-like orbitals, which are delocalized primarily about the

CE (***C***, ***D***, ***H***) and diaminoalkane (***E***, ***F***, ***G***) moieties. Noteworthy are the very low excitation energies that indicate that some of the low excited states rovibrational envelopes overlap and are populated by electron capture or transfer. Note that only the ***X*** state of $\text{RE}_\text{v} = 5.08\,\text{eV}$ is near resonant with electron transfer from Na, while the ***E*** through ***G*** states of $\text{RE}_\text{v} = 5.08 - 1.15 = 3.93\,\text{eV}$ are near resonant with electron transfer from Cs.

Table 3
Dissociation energies

Reaction	Energy[a]	
	B3LYP 6-31+(+)G (d,p)[b]	B3-PMP2 6-311++G (2d,p)
$\boldsymbol{7}\text{-1CE}^{+} \rightarrow \boldsymbol{7}^{+} + \text{CE}$	174	189
$\boldsymbol{7}\text{-1CE}^{+} \rightarrow \boldsymbol{7a}\text{-1CE}^{+}$	35	24
$\boldsymbol{7}\text{-1CE}^{2+} \rightarrow \boldsymbol{7}^{2+} + \text{CE}$	270	287
$\boldsymbol{7}\text{-1CE}^{2+} \rightarrow \boldsymbol{7}^{+} + (\text{CE} + \text{H})^{+}$	13	25
$\boldsymbol{7}\text{-1CE}^{\bullet+} \rightarrow \boldsymbol{7}^{\bullet+} + \text{CE}$	176	220
$(\text{CE} + \text{H})^{\bullet} \rightarrow \text{CE} + \text{H}^{\bullet}$	–135	–156
$\text{CH}_3\text{NH}_3{}^{+}\cdot\text{CE} \rightarrow \text{CH}_3\text{NH}_3{}^{+} + \text{CE}$	263	273
$[\text{CH}_3\text{NH}_3\cdot\text{CE}]^{\bullet} \rightarrow \text{CH}_3\text{NH}_3{}^{\bullet} + \text{CE}$	11	35
$\boldsymbol{4}\text{-1CE}^{\bullet+} \rightarrow \boldsymbol{4}\text{-1CE}^{+} + \text{H}^{\bullet}$	–6	–28
$\boldsymbol{5}\text{-1CE}^{\bullet+} \rightarrow \boldsymbol{5}\text{-1CE}^{+} + \text{H}^{\bullet}$	–10	–25
$\boldsymbol{7}\text{-1CE}^{\bullet+} \rightarrow \boldsymbol{7}\text{-1CE}^{+} + \text{H}^{\bullet}$	–11	–37
$\boldsymbol{7}^{\bullet+} \rightarrow \textbf{TS}(\text{N—H})_{\text{diss}}$	49	23
$\boldsymbol{7}^{\bullet+} \rightarrow \boldsymbol{7}^{+} + \text{H}^{\bullet}$	–18	–69
$\boldsymbol{7}^{\bullet+} \rightarrow \boldsymbol{7a}^{\bullet+}$	–21	–47
$\boldsymbol{7}^{\bullet+} \rightarrow \textbf{TS}(\text{C—C})_{\text{rot}}$	13	13
$\boldsymbol{12}^{\bullet+} \rightarrow \boldsymbol{12}^{+} + \text{H}^{\bullet}$	2	–17
$\boldsymbol{12}^{\bullet+} \rightarrow \boldsymbol{12a}^{+} + \text{H}^{\bullet}$	–5	–67
$\boldsymbol{12a}^{\bullet+} \rightarrow \boldsymbol{12a}^{+} + \text{H}^{\bullet}$	2	–17

[a] In units of kJ mol^{-1}. Including zero-point vibrational energies and referring to 0 K.

[b] Calculations with the 6-31+G(d,p) and 6-31++G(d,p) basis sets for cations and radicals, respectively.

3.7. *Discussion of ECD and ECID*

The dissociations upon electron capture and transfer share some common features but also show differences. In discussing these, one has to realize the different experimental conditions for ECD and ECID. In ECD, the charge-reduced ion receives the entire recombination energy that, in combination with the ion thermal energy, drives dissociations that are observed on a millisecond to second time scale. In ECID, the charge-reduced ion receives internal energy which is due to a difference between the recombination energy to the electronic state of the incipient radical and the ionization energy of the alkali metal atom. In addition, a fraction of the non-conserved COM collision energy, $T_\text{CM} = 3\text{–}15\,\text{keV}$, can be transferred to the charge-reduced ion to drive high-energy dissociations. The ECID dissociations occur on the experimental time scale of 3–9 μs.

ECID of free diaminoalkane ions results primarily in loss of an H atom and minor elimination of ammonia. This behavior is consistent with the dissociation thermochemistry and kinetics of other alkane ammonium hypervalent radicals [3f–n]. For example, loss of H from $\boldsymbol{7}^{\bullet+}$ is $69\,\text{kJ mol}^{-1}$ exothermic and requires an energy barrier of $23\,\text{kJ mol}^{-1}$ in the ***X*** electronic state (Table 3). The low barrier allows for an extremely fast dissociation, considering the excitation (E_exc) due to electron transfer, e.g., $E_\text{exc} = \text{RE}(\boldsymbol{7}^{2+}) - \text{IE(Na)} = 56\,\text{kJ mol}^{-1}$. Because of the absence of Coulomb repulsion, the charge-reduced ion $\boldsymbol{7}^{\bullet+}$ can competitively fold to conformer $\boldsymbol{7a}^{\bullet+}$ ($\Delta H_{\text{rxn},0}$ ($\boldsymbol{7}^{\bullet+} \rightarrow \boldsymbol{7a}^{\bullet+}$) = $-47\,\text{kJ mol}^{-1}$) through a sequence of low-energy transition states (Scheme 2) and eliminate an ammonium hydrogen atom from $\boldsymbol{7a}^{\bullet+}$ or one of the intermediates. Complete dissociation also occurs with $\boldsymbol{12}^{\bullet+}$ where the loss of H is exothermic by $\Delta H_{\text{rxn},0} = -17\,\text{kJ mol}^{-1}$ and can be driven by the rovibrational thermal energy of the precursor ion, e.g., H_rovib ($\boldsymbol{12}^{2+}$) = $48\,\text{kJ mol}^{-1}$ at 298 K. Loss of ammonia, albeit also highly exothermic [3m], is known to have higher energy barriers than loss of *H* and is kinetically disfavored in the ***X*** states of ammo-

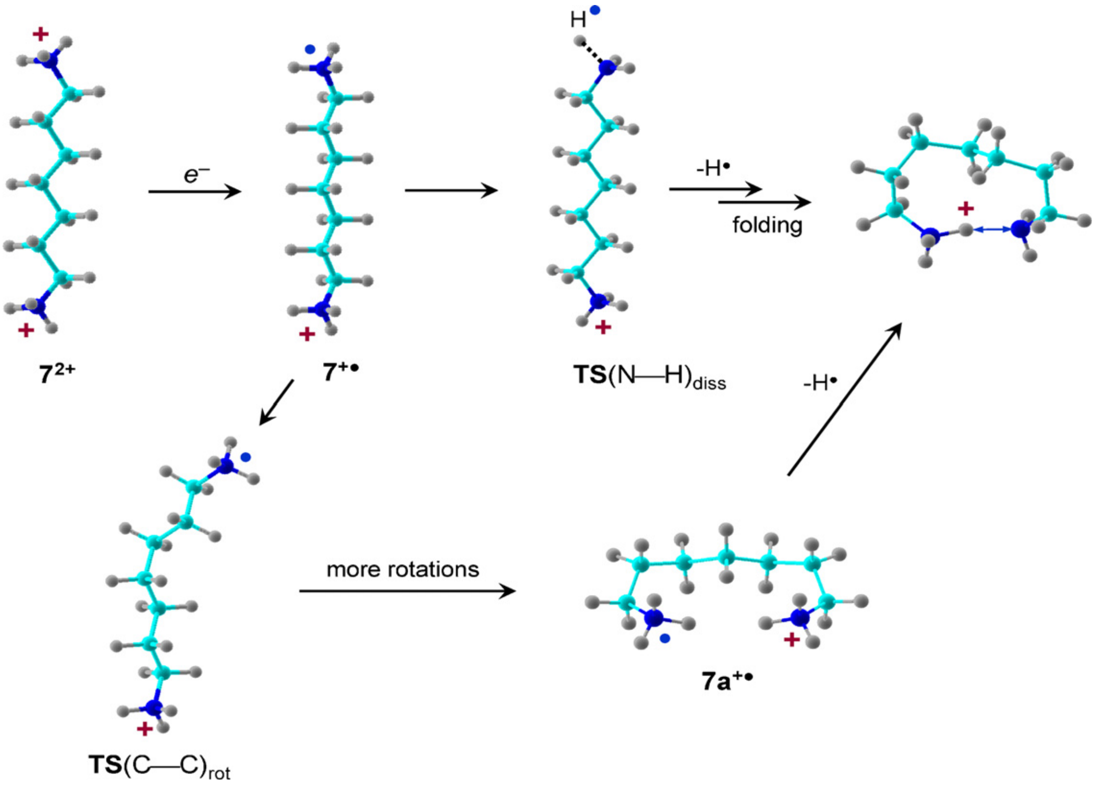

Scheme 2.

nium radicals. The presence of the chain fragments is remarkable, because they must be formed by highly endothermic C—C bond dissociations. These minor dissociations probably occur from excited electronic states of charge reduced ***7***$^{\bullet+}$ and ***12***$^{\bullet+}$ that are accessed upon keV collisions with both Na and Cs, by analogy with dissociations of 1,*n*-diaminoalkane radicals reported previously [3l].

Both ECD and ECID of the diaminoalkane·CE complexes result in the loss of an H atom (M^+ ions) combined with the loss of the crown ether ligand (A^+ ions). However, there are major differences in the relative intensities of these fragments. In ECID, a major fraction of M^+ survive to be detected and, in fact, represent the most abundant charge-reduced species. In ECD, the majority of M^+ dissociate to form A^+. A loss of an ammonium H atom resulting from electron capture by the outer ammonium group can proceed from the ground electronic state of the charge-reduced complex. The dissociation by H atom loss is exothermic, e.g., ($\Delta H_{\mathrm{rxn},0} = -37\,\mathrm{kJ\,mol^{-1}}$) for the charge-reduced intermediate ***7***-1CE$^{\bullet+}$. In contrast, loss of CE from ***7***-1CE$^{\bullet+}$ is calculated to be $>200\,\mathrm{kJ\,mol^{-1}}$ endothermic, indicating strong H-bonding between the CE and the coordinated ammonium group.

Dissociation of M^+ by loss of a neutral CE molecule is also endothermic, e.g., $\Delta H_{\mathrm{rxn},0} = 189\,\mathrm{kJ\,mol^{-1}}$ for ***7***-1CE$^+$. This energy can be readily supplied by electron-ion recombination (RE(***7***-1CE^{2+}) = 5.12 eV = 494 kJ mol^{-1}), but not by resonant electron transfer from Na or Cs alone where the ion excitation is $<114\,\mathrm{kJ\,mol^{-1}}$ if formed in the ground electronic state. This indicates that the dissociating fraction of M^+ must have been formed from an excited electronic state of charge-reduced ***7***-1CE$^{\bullet+}$ that was accessed by the keV collision. Formation of excited electronic states would also account for the different extent of M^+ dissociation following electron transfer from Na and Cs. Nevertheless, the fact that the nominally more exothermic electron transfer from Cs results in less extensive dissociation is puzzling. One possible explanation is that the hydrogen atom eliminated from the ***E*** through ***G*** states of ***7***-1CE$^{\bullet+}$, which are near resonant with electron transfer from Cs, departs with substantial kinetic energy leaving the M^+ ion with less internal energy. There are no calculated electronic excited states that are near resonant for Na. Similarly, ejection of a kinetically excited H atom upon electron capture by small clusters of $[\mathrm{Mg(H_2O)}_n]^{2+}$ has been recently observed [13].

Finally, it should be noted that cross-sections for femtosecond electron transfer depend on the Franck–Condon factors for the particular electronic state of the incipient charge-reduced species and thus the population of electronic states may be different for different electron donors and also different from that accessed by capture of a low-energy free electron. This and the very different time scales for dissociation explain the principal differences in the relative intensities of the primary (M^+) and secondary (A^+) product ions in ECD and ECID.

The ECD and ECID spectra of diaminoalkane ion complexes with two CE ligands also show similarities and differences. The main fragments in both kinds of spectra are due to loss of H and one CE molecule to form stable M^+. While facile loss of H is intrinsic to the reduced ammonium group [3f–n], the loss of the CE ligand is presumably due to its weakened bonding to the neutral NH_3 and/or NH_2 groups. Further dissociation proceeds by loss of the remaining stronger bound CE molecule to yield A^+ ions. The differences in CE binding to ammonium cations and radicals are documented by the substantially different dissociation energies for the $[\mathrm{CH_3NH_3}^+\cdot\mathrm{CE}]$ ion and $[\mathrm{CH_3NH_3}\cdot\mathrm{CE}]^\bullet$ neutral complexes, $\Delta H_{\mathrm{rxn}} = 273$ and $35\,\mathrm{kJ\,mol^{-1}}$, respectively (Table 3). The main difference between the ECD and ECID spectra is the presence in the latter of the ion series due to C—C bond cleavages in the diaminoalkane chain. These dissociations correspond to high-energy processes that likely originate from excited electronic states accessed by collisional electron transfer, but not upon capture of a free electron.

4. Conclusions

This comparative study of ECD and ECID of model ammonium dications points to different energies and time scales in dissociations triggered by electron capture and fast collisional electron transfer. The main dissociation due to loss of an ammonium hydrogen atom occurs in both ECD and ECID. However, the spectra substantially differ in the consecutive dissociations by loss of the CE ligand. In addition, the ECID spectra show unique minor dissociations that can be assigned to the formation of different electronic states upon charge reduction. The CE ligand is found to have a substantial effect on the recombination energy of the ammonium cation and also affects the electronic properties of the charge-reduced cation-radical species.

Acknowledgements

FT thanks the National Science Foundation for support through grants CHE-0349595 and CHE-0750048 for experiments and CHE-0342956 for computations, and the University of Aarhus, Denmark for a Visiting Professor fellowship in June–August 2007. ERW thanks the National Science Foundation (CHE-041593 and CHE-0718790) and the University of Aarhus, Denmark, for a visiting professor fellowship in 2005, and AISH gratefully acknowledges the funding from the European Project ITS-LEIF (RII 3/02 6016).

Appendix A. Supplementary data

Supplementary data associated with this article can be found, in the online version, at doi:10.1016/j.ijms.2008.04.021.

References

[1] (a) G.B. Lewis, J. Am. Chem. Soc. 38 (1916) 762;
(b) A.E. Reed, P.v.R. Schleyer, J. Am. Chem. Soc. 112 (1990) 1434.
[2] (a) A. Schuster, Br. Assoc. Adv. Sci. Rep. (1872) 38;
(b) G. Hezberg, Discuss. Faraday Soc. 71 (1981) 165;
(c) F. Alberti, K.P. Huber, J.K.G. Watson, J. Mol. Spectrosc. 107 (1984) 133;
(d) K. Fuke, R. Takasu, F. Misaizu, Chem. Phys. Lett. 229 (1994) 597;
(e) N. Okai, A. Takahata, K. Fuke, Chem. Phys. Lett. 386 (2004) 442.
[3] (a) B.W. Williams, R.F. Porter, J. Chem. Phys. 73 (1980) 5598;
(b) G.I. Gellene, D.A. Cleary, R.F. Porter, J. Chem. Phys. 77 (1982) 3471;
(c) G.I. Gellene, R.F. Porter, Acc. Chem. Res. 16 (1983) 200;
(d) C. Wesdemiotis, P.O. Danis, R. Feng, J. Tso, F.W. McLafferty, J. Am. Chem. Soc 107 (1985) 8059;
(e) S. Beranova, C. Wesdemiotis, Int. J. Mass Spectrom. Ion Process. 134 (1994) 83;
(f) V.Q. Nguyen, M. Sadilek, A.J. Frank, J.G. Ferrier, F. Tureček, J. Phys. Chem. A 101 (1997) 3789;
(g) S.A. Shaffer, F. Tureček, J. Am. Chem. Soc. 116 (1994) 8647;
(h) L. Frøsig, F. Tureček, J. Am. Soc. Mass Spectrom. 9 (1998) 242;
(i) J.K. Wolken, F. Tureček, J. Mass Spectrom. 32 (1997) 1162;
(j) S.A. Shaffer, M. Sadilek, F. Tureček, J. Org. Chem. 61 (1996) 5234;
(k) S.A. Shaffer, J.K. Wolken, F. Tureček, J. Am. Soc. Mass Spectrom. 8 (1997) 1111;
(l) S.A. Shaffer, F. Tureček, J. Am. Soc. Mass Spectrom. 6 (1995) 1004;
(m) M. Sadilek, F. Turecek, Chem. Phys. Lett. 263 (1996) 203;
(n) C. Yao, F. Turecek, F. Phys. Chem. Chem. Phys. 7 (2005) 912.
[4] (a) S. Raynor, D.R. Hershbach, J. Phys. Chem. 86 (1982) 3592;
(b) S. Havriliak, H.F. King, J. Am. Chem. Soc. 105 (1983) 4;
(c) H. Cardy, D. Kiotard, A. Dargelos, E. Poquet, Chem. Phys. 77 (1983) 287;
(d) E. Kassab, E. Evleth, J. Am. Chem. Soc. 109 (1987) 1653;
(e) I. Martin, A.C. Lavin, M. Velasco, M.O. Martin, J. Karwowski, G.H.F. Diercksen, Chem. Phys. 202 (1996) 307;
(f) A.I. Boldyrev, J. Simons, J. Chem. Phys. 97 (1992) 6621.
[5] (a) R.A. Zubarev, N.L. Kelleher, F.W. McLafferty, J. Am. Chem. Soc. 120 (1998) 3265;
(b) K. Breuker, H.B. Oh, D.M. Horn, B.A. Cerda, F.W. McLafferty, J. Am. Chem. Soc. 124 (2002) 6407;

(c) K. Breuker, H.B. Oh, C. Lin, B.K. Carpenter, F.W. McLafferty, Proc. Natl. Acad. Sci. U.S.A. 101 (2004) 14011;
(d) E.W. Robinson, R.D. Leib, E.R. Williams, J. Am. Soc. Mass Spectrom. 17 (2006) 1469;
(e) A. Stensballe, O.N. Jensen, J.V. Olsen, K.F. Hasselmann, R.A. Zubarev, Rapid Commun. Mass Spectrom. 14 (2000) 1793;
(f) E. Mirgorodskaya, P. Roepstorff, R.A. Zubarev, Anal. Chem. 71 (1999) 4431;
(g) S.K. Sze, Y. Ge, H.B. Oh, F.W. McLafferty, Proc. Natl. Acad. Sci. U.S.A. 99 (2002) 1774;
(h) N.L. Kelleher, R.A. Zubarev, K. Bush, B. Furie, B.C. Furie, F.W. McLafferty, C.T. Walsh, Anal. Chem. 71 (1999) 4250;
(i) Y. Ge, B.G. Lawhorn, M. ElNaggar, E. Strauss, J.H. Park, T.P. Begley, F.W. McLafferty, J. Am. Chem. Soc. 124 (2002) 672;
(j) H.J. Cooper, K. Håkansson, A.G. Marshall, Mass Spectrom. Rev. 24 (2005) 201.

[6] (a) A.I.S. Holm, P. Hvelplund, U. Kadhane, M.K. Larsen, B. Liu, S.B. Nielsen, S. Panja, J.M. Pedersen, T. Skrydstrup, K. Støchkel, E.R. Williams, E.S. Worm, J. Phys. Chem. A 111 (2007) 9641;
(b) T. Chakraborty, A.I.S. Holm, P. Hvelplund, S.B. Nielsen, J.-C. Poully, E.S. Worm, E.R. Williams, J. Am. Soc. Mass Spectrom. 17 (2006) 1675;
(c) P. Hvelplund, B. Liu, S. Brøndsted Nielsen, S. Tomita, Int. J. Mass Spectrom. 225 (2003) 83.

[7] (a) J.E.P. Syka, J.J. Coon, M.J. Schroeder, J. Shabanowitz, D.F. Hunt, Proc. Natl. Acad. Sci. U.S.A. 101 (2004) 9528;
(b) J.J. Coon, J.E.P. Syka, J.C. Schwartz, J. Shabanowitz, D.F. Hunt, Int. J. Mass Spectrom. 236 (2004) 33;
(c) J.J. Coon, B. Ueberheide, J.E.P. Syka, D.D. Dryhurst, J. Ausio, J. Shabanowitz, D.F. Hunt, Proc. Natl. Acad. Sci. U.S.A. 102 (2005) 9463;
(d) S.J. Pitteri, P.A. Chrisman, J.M. Hogan, S.A. McLuckey, Anal. Chem. 77 (2005) 1831;
(e) H.P. Gunawardena, M. He, P.A. Chrisman, S.J. Pitteri, J.M. Hogan, B.D. Hodges, S.A. McLuckey, J. Am. Chem. Soc. 127 (2005) 12627;
(f) R. Srikanth, J. Wilson, J.D. Bridgewater, J.R. Numbers, J. Lim, M.R. Olbris, A. Kettani, R.W. Vachet, J. Am. Chem. Soc. Mass Spectrom. 18 (2007) 1499.

[8] (a) S.W. Lee, H.N. Lee, H.S. Kim, J.L. Beauchamp, J. Am. Chem. Soc. 120 (1998) 5800;
(b) R.R. Julian, J.L. Beauchamp, Int. J. Mass Spectrom. 210/211 (2001) 613.

[9] T. Ly, R.R. Julian, J. Am. Soc. Mass Spectrom. 17 (2006) 1209.

[10] J.J. Wilson, G.J. Kirkovits, J.L. Sessler, J.S. Brodbelt, J. Am. Soc. Mass Spectrom. 19 (2008) 257.

[11] J.C. Jurchen, E.R. Williams, J. Am. Chem. Soc. 125 (2003) 2817.

[12] M.F. Bush, J.T. O'Brien, J.S. Prell, R.J. Saykally, E.R. Williams, J. Am. Chem. Soc 129 (2007) 1612.

[13] R.D. Leib, W.A. Donald, M.F. Bush, J.T. O'Brien, E.R. Williams, J. Am. Soc. Mass Spectrom. 18 (2007) 1217.

[14] (a) O.V. Boltalina, P. Hvelplund, T.J.D. Jørgensen, M.C. Larsen, M.O. Larsson, D.A. Sharoitchenko, M. Sørensen, Phys. Rev. A 62 (2000) 023202;
(b) M.O. Larsson, P. Hvelplund, M.C. Larsen, H. Shen, H. Cederquist, H.T. Schmidt, Int. J. Mass Spectrom. 177 (1998) 51.

[15] M.J. Frisch, G.W. Trucks, H.B. Schlegel, G.E. Scuseria, M.A. Robb, J.R. Cheeseman, J.A. Montgomery, Jr., T. Vreven, K.N. Kudin, J.C. Burant, J.M. Millam, S.S. Iyengar, J. Tomasi, V. Barone, B. Mennucci, M. Cossi, G. Scalmani, N. Rega, G.A. Petersson, H. Nakatsuji, M. Hada, M. Ehara, K. Toyota, R. Fukuda, J. Hasegawa, M. Ishida, T. Nakajima, Y. Honda, O. Kitao, H. Nakai, M. Klene, X. Li, J.E. Knox, H.P. Hratchian, J.B. Cross, C. Adamo, J. Jaramillo, R. Gomperts, R.E. Stratmann, O. Yazyev, A.J. Austin, R. Cammi, C. Pomelli, J.W. Ochterski, P.Y. Ayala, K. Morokuma, G.A. Voth, P. Salvador, J.J. Dannenberg, V.G. Zakrzewski, S. Dapprich, A.D. Daniels, M.C. Strain, O. Farkas, D.K. Malick, A.D. Rabuck, K. Raghavachari, J.B. Foresman, J.V. Ortiz, Q. Cui, A.G. Baboul, S. Clifford, J. Cioslowski, B.B. Stefanov, G. Liu, A. Liashenko, P. Piskorz, I. Komaromi, R.L. Martin, D.J. Fox, T. Keith, M.A. Al-Laham, C.Y. Peng, A. Nanayakkara, M. Challacombe, P.M.W. Gill, B. Johnson, W. Chen, M.W. Wong, C. Gonzalez, J.A. Pople, J.A. Gaussian 03, Revision B.05; Gaussian, Inc.; Pittsburgh PA, 2003.

[16] (a) A.D. Becke, J. Chem. Phys. 98 (1993) 1372;
(b) A.D. Becke, J. Chem. Phys. 98 (1993) 5648;
(c) P.J. Stephens, F.J. Devlin, C.F. Chabalowski, M.J. Frisch, J. Phys. Chem. 98 (1994) 11623.

[17] G. Rauhut, P. Pulay, J. Phys. Chem. 99 (1995) 3093.

[18] (a) H.B. Schlegel, J. Chem. Phys. 84 (1986) 4530;
(b) I. Mayer, Adv. Quantum Chem. 12 (1980) 189.

[19] (a) F. Tureček, J. Phys. Chem. A 102 (1998) 4703;
(b) F. Tureček, M. Polášek, A.J. Frank, M. Sadílek, J. Am. Chem. Soc. 122 (2000) 2361;
(c) M. Polášek, F. Tureček, J. Am. Chem. Soc. 122 (2000) 9511;
(d) F. Tureček, C. Yao, J. Phys. Chem. A 107 (2003) 9221;
(e) P.R. Rablen, J. Am. Chem. Soc. 122 (2000) 357;
(f) P.R. Rablen, J. Org. Chem. 65 (2000) 7930;
(g) P.R. Rablen, K.H. Bentrup, J. Am. Chem. Soc. 125 (2003) 2142;
(h) M. Hirama, T. Tokosumi, T. Ishida, J. Aihara, Chem. Phys. 305 (2004) 307.

[20] R.E. Stratmann, G.E. Scuseria, M.J. Frisch, J. Chem. Phys. 109 (1998) 8218.

[21] A.E. Reed, R.B. Weinstock, F. Weinhold, J. Chem. Phys. 83 (1985) 735.

[22] (a) D.S. Gross, S.E. Rodriguez-Cruz, S. Bock, E.R. Williams, J. Phys. Chem. 99 (1995) 4034;
(b) E.R. Williams, J. Mass Spectrom. 31 (1996) 831.

[23] (a) NIST Standard Reference Database Number 69, June, 2005 Release; http://webbook.nist.gov/chemistry;
(b) E.P. Hunter, S.G. Lias, J. Phys. Chem. Ref. Data 3 (1998) 413.

[24] M. Meot-Ner (Mautner), J. Am. Chem. Soc. 105 (1983) 4906.

[25] V.Q. Nguyen, F. Tureček, J. Mass Spectrom. 31 (1996) 843.

[26] (a) R.D. Leib, W.A. Donald, J.T. O'Brien, M.F. Bush, E.R. Williams, J. Am. Chem. Soc. 129 (2007) 7717;
(b) R.D. Leib, W.A. Donald, M.F. Bush, J.T. O'Brien, E.R. Williams, J. Am. Chem. Soc. 129 (2007) 4894;
(c) W.A. Donald, R.D. Leib, J.T. O'Brien, M.F. Bush, E.R. Williams, J. Am. Chem. Soc. (2008), doi:10.1021/ja073946i.

[27] F. Tureček, Top. Curr. Chem. 225 (2003) 77.

[28] E.A. Syrstad, F. Tureček, J. Am. Soc. Mass Spectrom. 16 (2005) 208.